Supplementary Information

Contents

Supplementary Information on Main Figures

Figure 1

(a) A significant interaction was observed between the effects of genotype (WT vs. *4E-BP2* KO) and the time spent in a chamber (Stranger 1, center, empty), $F(2,72)=77.12$, $p<0.001$. WT mice spent significantly more time with the novel mouse (506±9.8s) than with the novel object (398±10.8s) ($p<0.001$). KO mice spent significantly less time with the novel mouse (395±9.5s) than with the novel object (450±7.5s) ($p<0.01$) and less time with the novel mouse than the WT mice ($p<0.02$). The interaction between genotype and time spent sniffing the novel mouse or object was also significant [$F(1,48)=251.12$, $p<0.001$]. WT (130±3.1s, $p<0.01$) and KO (56±3.4s, $p<0.02$) mice spent more time sniffing the novel mouse than the novel object (WT: 14±7.8s, KO: 12±6.7s), but WT mice spent significantly more time than the KO mice ($p<0.01$). The interaction between the number of entries and the two side chamber types was also significant [$F(1,48)=8.36$, $p=0.006$]. KO mice entered significantly less times (19.5±1.3) in the Stranger 1 compartment ($p<0.02$) as compared to WT (26.5±2.3), while entries in the empty wire-cage compartment were comparable between animal genotypes (WT: 24.25±3.4, $p=0.673$; KO, 24.9±5.2, $p=0.080$)

(b) Pairs of WT-KO (125±1.9s, $p=0.010$) or KO-KO (99±3.2s, $p=0.023$) interact for a shorter period of time, as compared to the WT-WT pair (245±2.3s), in a 20-min home-cage recording session. Total number of interaction events is reduced in the KO-KO pairs (11±4.2) as compared to WT-WT (25±4.8, $p=0.028$) or WT-KO (23±3.8, $p=0.021$) pairs.

(c) The KO-WT (72±19.9s, $p=0.023$), KO-KO (80±12.3s, $p=0.022$) pairs interacted for a shorter period of time, as compared to the WT-WT pair (125±12.9s) in a 10 min session. The number of contact events is significantly reduced in the KO-KO (18±3.2) vs WT-WT(34±2.3, $p=0.026$) or WT-KO(36±1.9, $p=0.022$) pairs.

(d) Increased self-grooming in *4E-BP2* KO mice. *4E-BP2* KO mice spend more time grooming (102±14) than WT mice (58±3.4) in a 10 min session ($p=0.022$).

(e) Repetitive/stereotyped behavior of *4E-BP2* KO mice in a marble-burying task. *4E-BP2 KO* mice buried significantly more marbles (WT8.2±0.8, KO13.4±1.2, $p=0.021$) than their WT littermates. For d-e, n=12 animals for each group; Student's t-test.

(f-h) Elevated USVs in *4E-BP2* KO pups as compared to WT at various post-natal days (pnd) (f) Increased number (pnd2: 47.5±7.5%, $p=0.035$; pnd4: 56±6.8%, $p=0.031$; pnd6: 64±12.6, $p=0.030$; pnd8: 63±11.1%, $p=0.029$; pnd12: 70.5±8.3%, $p=0.023$) and (g) increased duration of calls (pnd2: 52±4.7%, $p=0.025$; pnd4: 58±4.1%, $p=0.029$; pnd6: 58±5.2%, $p=0.032$; pnd8: 59±4.5%, $p=0.029$; pnd12: 61±6.8%, $p=0.027$).

(h) Increased amplitude (in decibel) of USVs for the *4E-BP2* KO animals (day 8: 34%±4.1; p=0.029 and day 12: 36%±4.2; p=0.032), as compared to WT littermates.

Figure 2
(g-h) For WT - *4E-BP2* KO increase: NLGN 1 (Cr. 38.3±6.1%, p=0.031; Syn. 35.8±1.4%, p=0.036), NLGN 2 (Cr. 44.9±4.8%, p=0.029; Syn. 48.9±2.6%, p=0.031), NLGN 3 (Cr. 44.2±7.2%, p=0.023; Syn. 32.1±2.6%, p=0.021), NLGN 4 (Cr. 43.1±4.8%, p=0.018; Syn. 28.2±1.6%, p=0.024); for WT - β-T*eIF4E* increase: NLGN 1 (Syn. 20.5±3.4%, p=0.017), NLGN 2 (Syn. 34.3±2.1%, p=0.014), NLGN 3 (Syn. 49.4±2.2%, p=0.013), NLGN 4 (Syn. 31.2±1.3%, p=0.021);

Figure 3
(b) Summary bar graphs showing increased mEPSC amplitude (35.9±9.5%, p=0.015) and frequency (105.9±22%, p=0.002) in *4E-BP2* KO neurons, as compared to WT neurons.
(d) Summary bar graphs illustrating the selective effect of *4E-BP2* KO on mIPSC amplitude (increase 48.5±15.3%, p=0.047) and no effect on frequency (p=0.367). Number of cells are indicated above bar.
(e) Bar graphs showing the increase in total charge transfer (cumulative sum of charge for all mEPSCs (84.9±31.7%, p=0.035) or mIPSCs (47.9±7.9%, p=0.001) over a 10 min period) in *4E-BP2* KO relative to WT slices.

Figure 4
(c) Effect of 4EGI-1 on miniature EPSCs in slices from WT and *4E-BP2* KO mice. 4EGI-1 treatment reverses the facilitation of mEPSC amplitude (TOP; p=0.031) and frequency (BOTTOM; p=0.020) in *4E-BP2* KO mice (WT-vehicle, 7.2±0.8pA and 3.9±0.4Hz; KO-vehicle, 10.2±0.4pA and 5.3±0.1Hz; KO-4EGI-1, 5.8±1.4pA and 3.2±0.5Hz).
(d) Effect of 4EGI-1 on miniature IPSCs in slices from WT and *4E-BP2* KO mice. 4EGI-1 treatment prevents the facilitation of mIPSC amplitude (TOP; p=0.024) without affecting frequency (BOTTOM; p=0.104) in *4E-BP2* KO mice (WT-vehicle, 20.4±0.6pA and 16.8±1.4Hz; KO-vehicle, 25.3±0.9pA and 16.7±1.3Hz; KO-4EGI-1, 19.1±1.5pA and 17.0±1.3 Hz).
(e) 4EGI-1 rescues the increase in total charge transfer of mEPSCs (TOP; WT-vehicle, 22.1±1.5pC; KO-vehicle, 45.5±1.2pC; KO-4EGI-1, 21.1±5.2pC) (KO-vehicle vs KO-4EGI-1 p=0.018) and mIPSCs (MIDDLE; WT-vehicle, 1700.7±91.23pC; KO-vehicle, 2234.7±82.1pC; KO-4EGI-1, 1820.2±113.7pC) (KO-vehicle vs KO-4EGI-1 p=0.031) in *4E-BP2* KO mice. BOTTOM: Comparison of relative increases in mEPSC and mIPSC total charge transfer, normalized to the mean WT value, for each neuron from *4E-BP2* KO slices. 4EGI-1 reduces the normalized charge transfer of mEPSCs and mIPSCs in *4E-BP2* KO mice. E (black), KO-vehicle mEPSC; E (gray), KO-4EGI-1 mEPSC; I (black), KO-vehicle mIPSC; I (gray), KO-4EGI-1 mIPSC. Kolmogorov-Smirnov tests: KO-vehicle E vs KO-4EGI-1 E, p=0.001, KS statistic=0.918; KO-vehicle I vs KO-4EGI-1 I, p=0.002, KS statistic=0.796.
For c-e, for mEPSCs and mIPSCs n=6 in each group; one-way ANOVA with Bonferroni's post-hoc; *corresponds to $p< 0.05$.
(f-g) Rescue effects of 4EGI-1 infusion in *4E-BP2* KO and WT mice in the three-chamber social interaction test. A significant interaction was observed between genotype,

time in a chamber and treatment [F(2,144)=323.67, p<0.001)]. *4E-BP2* KO mice treated with 4EGI-1 spent more time (472±11.1s, p=0.021) in the Stranger 1 compartment (c), and spent more time (88±3.2s, p=0.020) sniffing the wire cage of Stranger 1 (e), as compared to vehicle infused KO mice (in chamber: 336±22.4s and interaction 42.1±6.5s respectively). The interaction between genotype and time spent sniffing the novel mouse or object was also significant [*F*(1,96)=26.43, p<0.001]. In WT mice 4EGI-1 infusion had no effect on social behavior compared to vehicle (Supplementary table 4).
For f-g, n=12 for all groups, two-way ANOVA, with a Bonferroni post-hoc t-test; *corresponds to p<0.03.

Figure 5
(c) Effect of *Nlgn1* or *Nlgn2* knockdown on miniature EPSCs in transfected pyramidal cells of slices from *4E-BP2* KO and WT mice. In cells transfected with scrambled siRNA, mEPSC amplitude (p=0.018) and frequency (p=0.028) are increased in *4E-BP2* KO relative to WT mice. *Nlgn1* knockdown rescues the facilitation of mEPSC amplitude (p=0.011) and frequency (p=0.027) in *4E-BP2* KO mice, while *Nlgn2* knockdown does not affect mEPSC amplitude (p=0.095) or frequency (p=0.211) (WT-si scrambled, 5.1±0.2pA and 4.1±0.2Hz; KO-si scrambled, 10.3±0.3pA and 6.4±0.2Hz; KO-si *Nlgn1*, 7.6±0.6pA and 4.9±0.2Hz; KO-si *Nlgn2,* 9.8±0.4pA and 6.7±0.3Hz).
(d) Effect of *Nlgn1* or *Nlgn2* knockdown on miniature IPSCs in slices from *4E-BP2* KO and WT mice. In cells transfected with scrambled siRNA, mIPSC amplitude (p=0.011) is increased in *4E-BP2* KO relative to WT mice. *Nlgn2* knockdown rescues the facilitation of mIPSC amplitude (p=0.016) without affecting frequency (p=0.062) in *4E-BP2* KO mice, while *Nlgn1* knockdown does not affect mIPSC amplitude (p=0.084) or frequency (p=0.077) (WT-si scrambled, 19.5±1.2pA and 13.4±1.3Hz; KO-si scrambled, 23.9±1.1pA and 13.1±0.9Hz; KO-si *Nlgn1*, 24.9±0.9pA and 13.5±1.2Hz; KO-si *Nlgn2,* 20.1±0.8pA and 12.9±1.1Hz).
(e) In *4E-BP2* KO mice, *Nlgn1* knockdown rescues the increase in total charge transfer of mEPSCs (p=0.013) but not mIPSCs (p=0.213), while si*Nlgn2* rectifies total charge transfer of mIPSCs (p=0.031), but not mEPSCs (p=0.165), as compared to cells transfected with scrambled siRNA (TOP: WT-si scrambled, 25.1±1.2pC; KO-si scrambled, 48.8±4.3pC; KO-si *Nlgn1*, 35.47±1.8pC; KO-si *Nlgn2*, 46.6±3.1pC) (MIDDLE: WT-si scrambled, 988.7±121.3pC; KO-si scrambled, 1547.1±86.9pC; KO-si *Nlgn1*, 1613.1±121.4pC; KO-si *Nlgn2*, 1354.6±77.6pC). BOTTOM: Comparison of relative increases in mEPSC and mIPSC total charge transfer, normalized to the mean WT value, for each neuron from *4E-BP2* KO slices. *Nlgn1* knockdown reduces the normalized charge transfer of mEPSCs but not mIPSCs in *4E-BP2* KO mice (left), whereas *Nlgn2* knockdown diminishes the normalized charge transfer of mIPSCs but not mEPSCs (right). E (black), KO-si scrambled mEPSC; E (gray), KO-si *Nlgn1* or *2* mEPSC; I (black), KO-si scrambled mIPSC; I (gray), KO-si *Nlgn1* or *2* mIPSC. Kolmogorov-Smirnov tests: KO-si scrambled E vs KO-si *Nlgn1* E, p=0.001, KS statistic=0.906; KO-si scrambled I vs KO-si *Nlgn1* I, p=0.084, KS statistic=0.824; KO-si scrambled E vs KO-si *Nlgn2* E, p=0.241, KS statistic=0.757; KO-si scrambled I vs KO-si *Nlgn2* I, p=0.001, KS statistic=0.913.
For c-e, for mEPSC and IPSC n=5 in each group; one-way ANOVA with Bonferroni's post-hoc; *corresponds to p<0.05

(f-g) Knockdown of *Nlgn1* partially rescues the social interaction deficits of *4E-BP2* KO mice, while knockdown of *Nlgn2* exacerbates the phenotype. A significant interaction was observed between genotype, chamber and treatment [$F(2,144)=198.37$, $p<0.001$) for *Nlgn1* knockdown. *4E-BP2* KO mice injected with shRNAs against *Nlgn1* spent more time (432±8.1s, $p<0.02$) in the Stranger 1 compartment and spent more time (79.2±5.2s, $p<0.02$) sniffing the wire cage of Stranger 1 (d), as compared to shCtrl infused KO mice (340±22.4s, 32.16±6.5s). A significant interaction was observed between genotype, chamber and treatment [$F(2,144)=127.32$, $p<0.001$] for *Nlgn2* knockdown. *4E-BP2* KO mice injected with shRNAs against *Nlg2* spent less time (214±11.5s, $p<0.02$) in the Stranger 1 compartment and spent less time (21±4, $p<0.02$) sniffing the wire cage of Stranger 1 (d), as compared to vehicle infused KO mice. In WT mice *Nlgn1* or *Nlgn2* knockdown had no effect on social behavior compared to non-targeting shRNA (Supplementary table 4). The interaction between genotype and time spent sniffing the novel mouse or object was also significant for the *Nlgn1* knockdown experiment [$F(1,96)=98.32$, $p<0.001$] and for the *Nlgn2* [$F(1,96)=211.91$, $p<0.001$].
For f-g, n=12 for all groups, two-way ANOVA, with a Bonferroni post-hoc t-test; *corresponds to $p<0.02$.

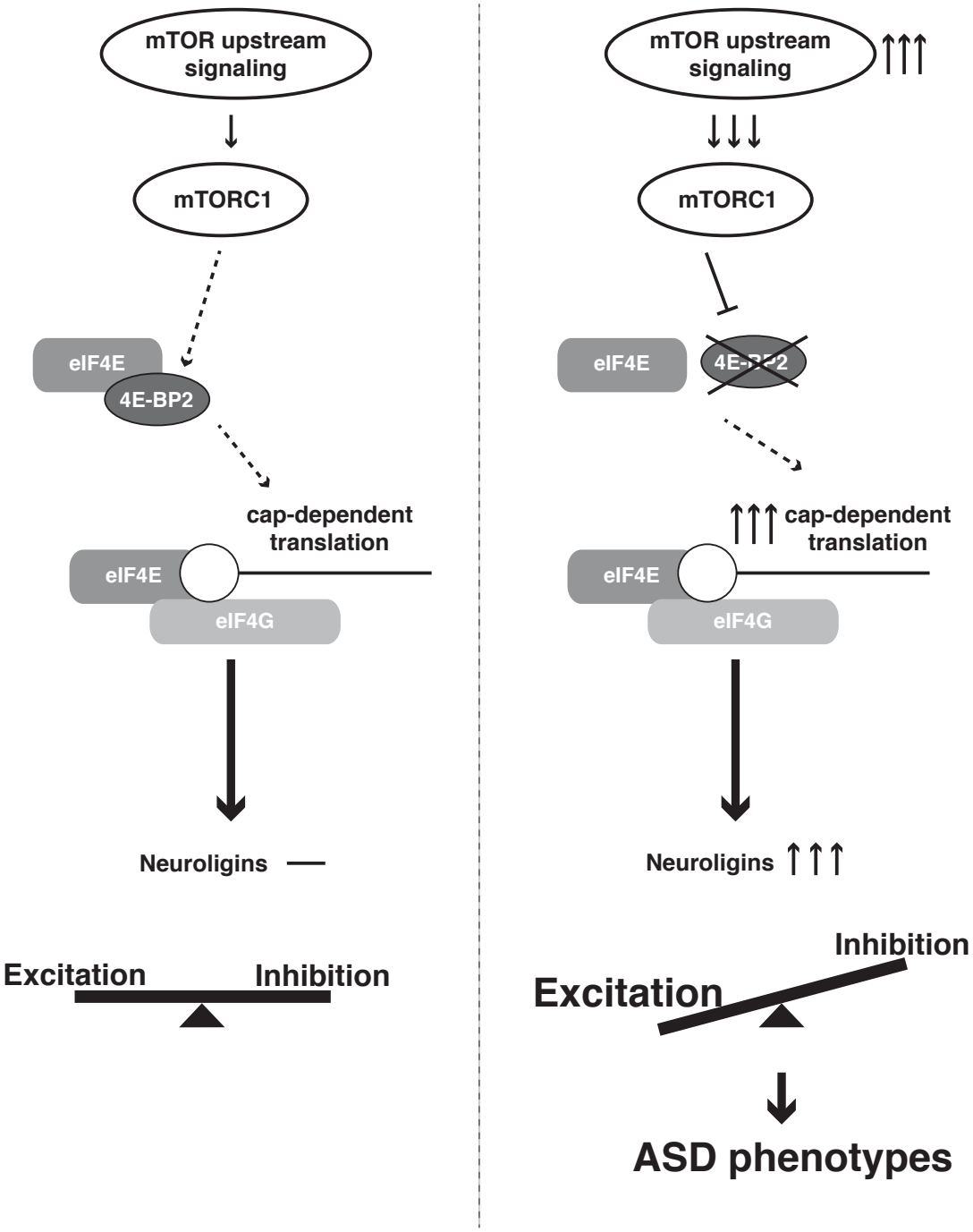

Supplementary Figure 1. Translational control of cap-dependent neuronal protein synthesis in ASD.
mTOR signaling integrates inputs from different sources. mTORC1 activation promotes the formation of the eIF4F initiation complex. 4E-BP2 inhibits translation by competing with eIF4G for eIF4E binding. Increased signaling leads to activation of mTORC1 and enhancement of cap-dependent translation. In *4E-BP2*-KO mice, increased translation of neuroligins, but not of PSD95 or other post-synaptic scaffolding molecules, shifts the balance towards synaptic excitation, which may lead to ASD phenotypes.

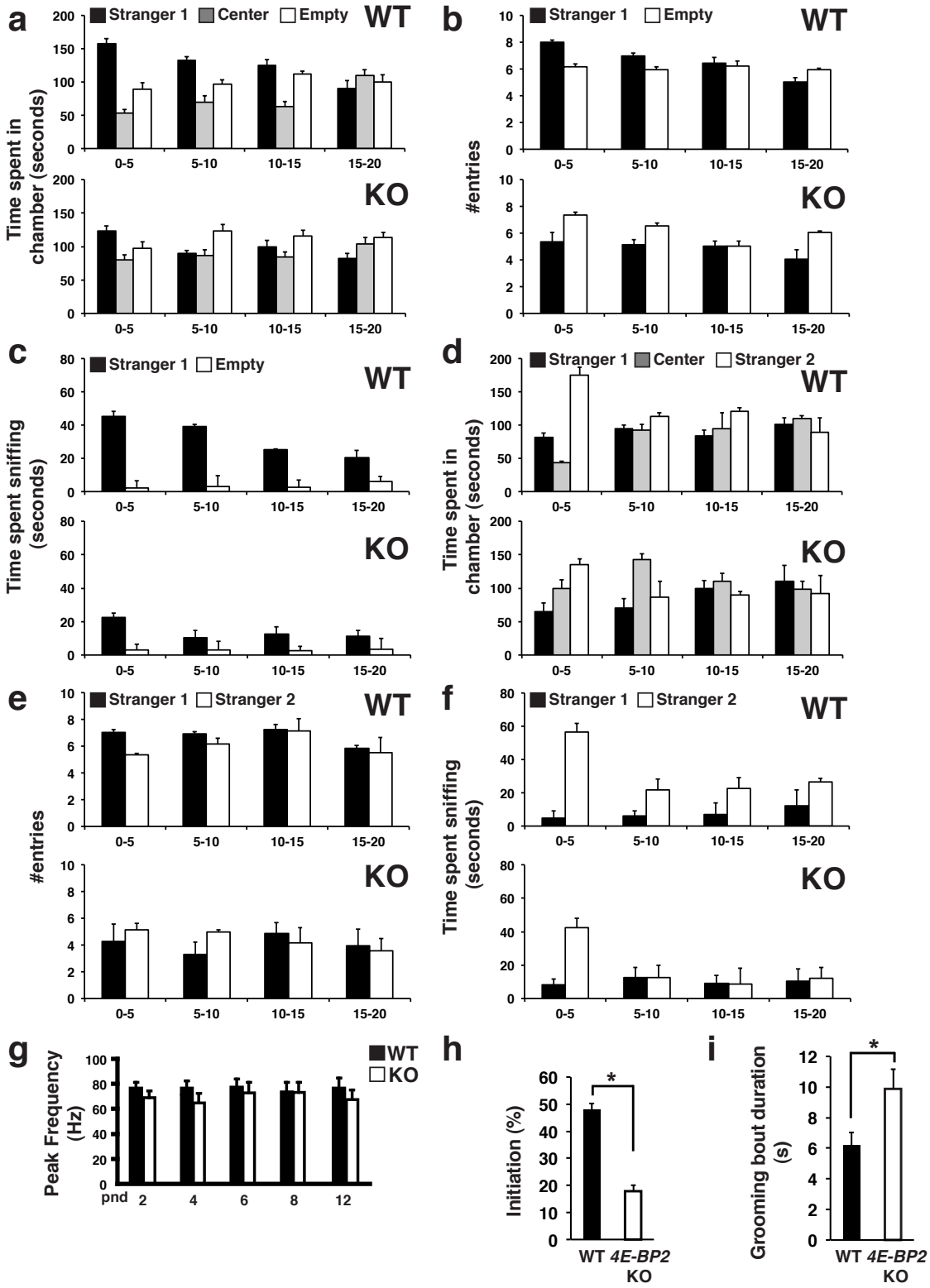

Supplementary Figure 2. Time-course analysis of the social interaction and preference for social novelty three-chamber arena tests in *4E-BP2* (WT or KO) mice, and additional data for main Figure 1.

Results are presented in 5 min time-bins.

(a) Time spent in the different chambers of the social arena in the social interaction test. In WT mice there is a progressive decrease in the interest of the test mouse for Stranger1, which is not observed in KO mice.
(b) Number of entries into the Stranger1 and empty chambers in the social interaction test. There is a progressive decline in the interest for Stranger1 in the WT but not KO test mice.
(c) Time spent sniffing the empty wire cage or that of Stranger1 in the social interaction test.
(d) Time spent in the different chambers of the social arena in the preference for social novelty test. More intense activity towards Stranger2 is observed in the 0-5 min time-bin.
(e) Number of entries into the Stranger1 and Stranger2 chambers in the preference for social novelty test.
(f) Time spent sniffing the Stranger1 or Stranger2 wire cage in the social interaction test. In the 0-5 min time-bin the test mice display the peak of their interest towards Stranger2.
For a-f, n=12; Two-way ANOVA with Bonferroni's post-hoc.
(g) Peak frequency (Hz) of pup USVs in WT and *4E-BP2*-KO mice. No differences are observed in the peak frequency (n=12, p=0.053); two-way ANOVA, with Bonferroni's post-hoc.
(h) Percentage of interactions initiated by WT (48±2.8) or *4E-BP2*-KO (18±2.6) mice in the homecage or openfield social interaction tests (p=0.018); n=12 animals for each group *p<0.03; Student's t-test.
(i) *4E-BP2*-KO mice engage in longer self-grooming bouts (9.9±1.2s) than WT littermates (6.2±0.8s) in a 10 min session (p=0.026); n=12 animals for each group *p<0.03; Student's t-test. All data are presented as mean ±SEM.

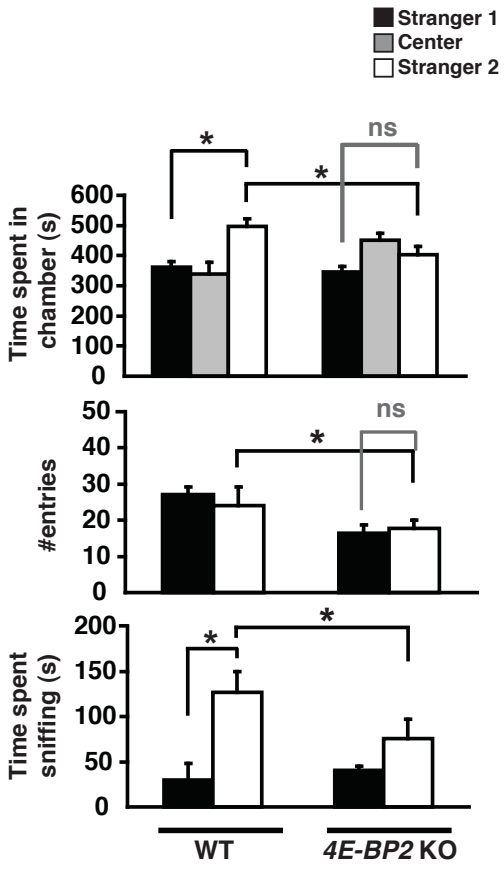

Supplementary Figure 3. Reduced Preference for social novelty in *4E-BP2*-KO mice. Reduced preference for social novelty in *4E-BP2*-KO compared to WT mice in a three-chamber arena test. A significant interaction was observed between genotype and time spent in a chamber type [$F(2,72)=81.4$, $p=0.002$] or time spent sniffing the familiar or novel mouse [$F(1,48)=35.4$, $p=0.002$] or number of entries in any of the side chambers [$F(1,48)=78.3$, $p=0.002$]; n=12 animals for each group; two-way ANOVA with Bonferroni's post-hoc, *$p<0.05$-statistics is Supplementary Table 4. All data are presented as mean ±SEM.

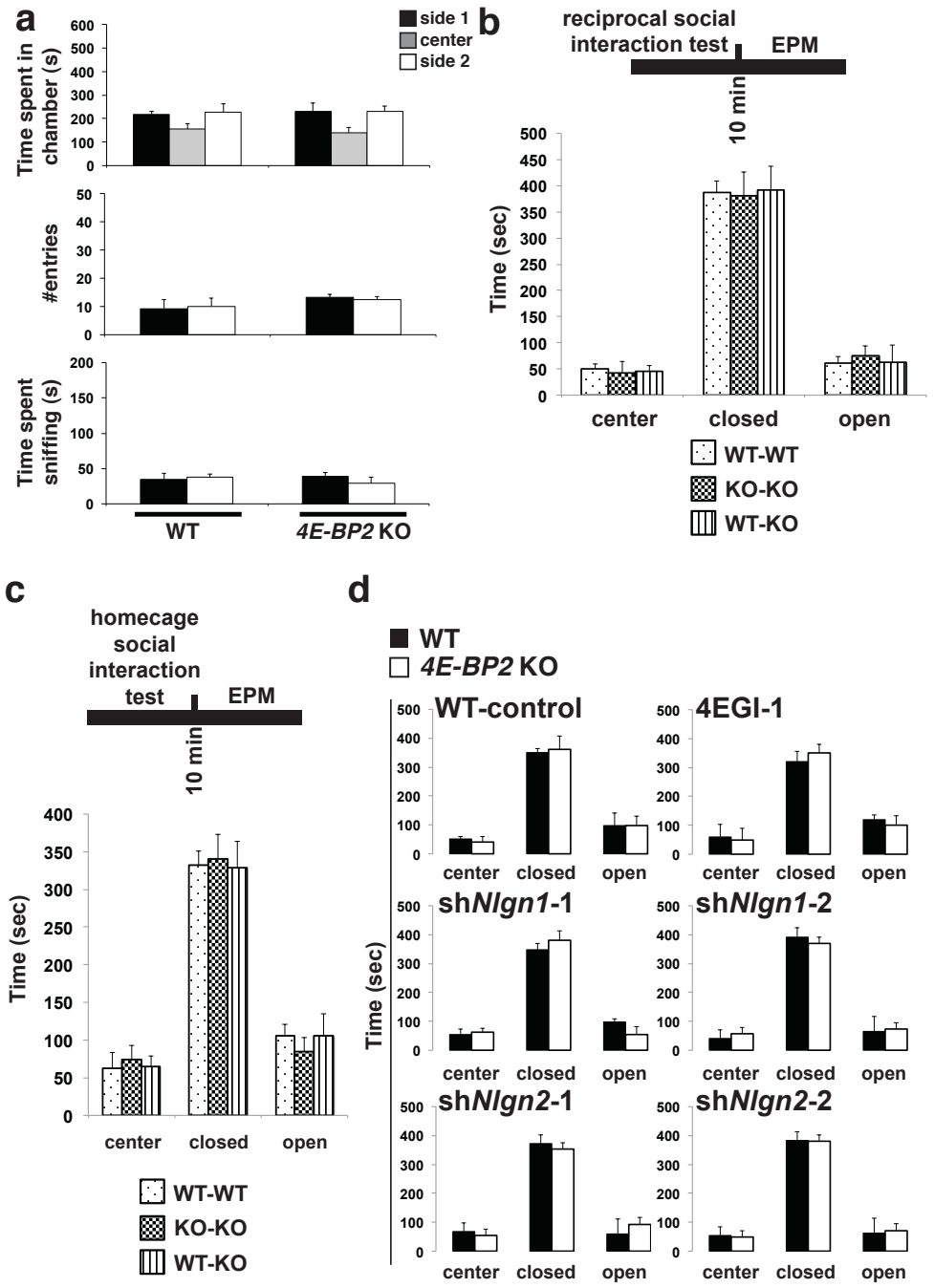

Supplementary Figure 4. Analysis of anxiety-related behaviors in *4E-BP2*-KO mice.
(a) No differences in time spent exploring the side chambers and number of entries in the initial habituation phase of the 3 chamber social approach test in *4E-BP2*-KO mice compared to WT (n=12), two-way ANOVA, with Bonferroni's post-hoc; statistics in Supplementary Table 4.
No differences in anxiety levels as assessed by the time spent in the center and open or closed arms of an Elevated Plus Maze, following reciprocal (b) or homecage (c) social

interaction tests in *4E-BP2*-KO mice compared to WT; (n=8) for each group-statistics in Supplementary Table 4.
(d) No differences in anxiety levels as assessed by the time spent in the center and open or closed arms of an Elevated Plus Maze, following the 3-chamber social approach test, between WT, *4E-BP2*-KO, 4EGI-1 infused (WT or KO), sh*Nlgn1-1,2* injected (WT or KO) or sh*Nlgn2-1,2* injected (WT or KO) mice; (n=8) for each group-statistics in Supplementary Table 4. Two-way ANOVA, with Bonferroni's post-hoc. All data are presented as mean ±SEM.

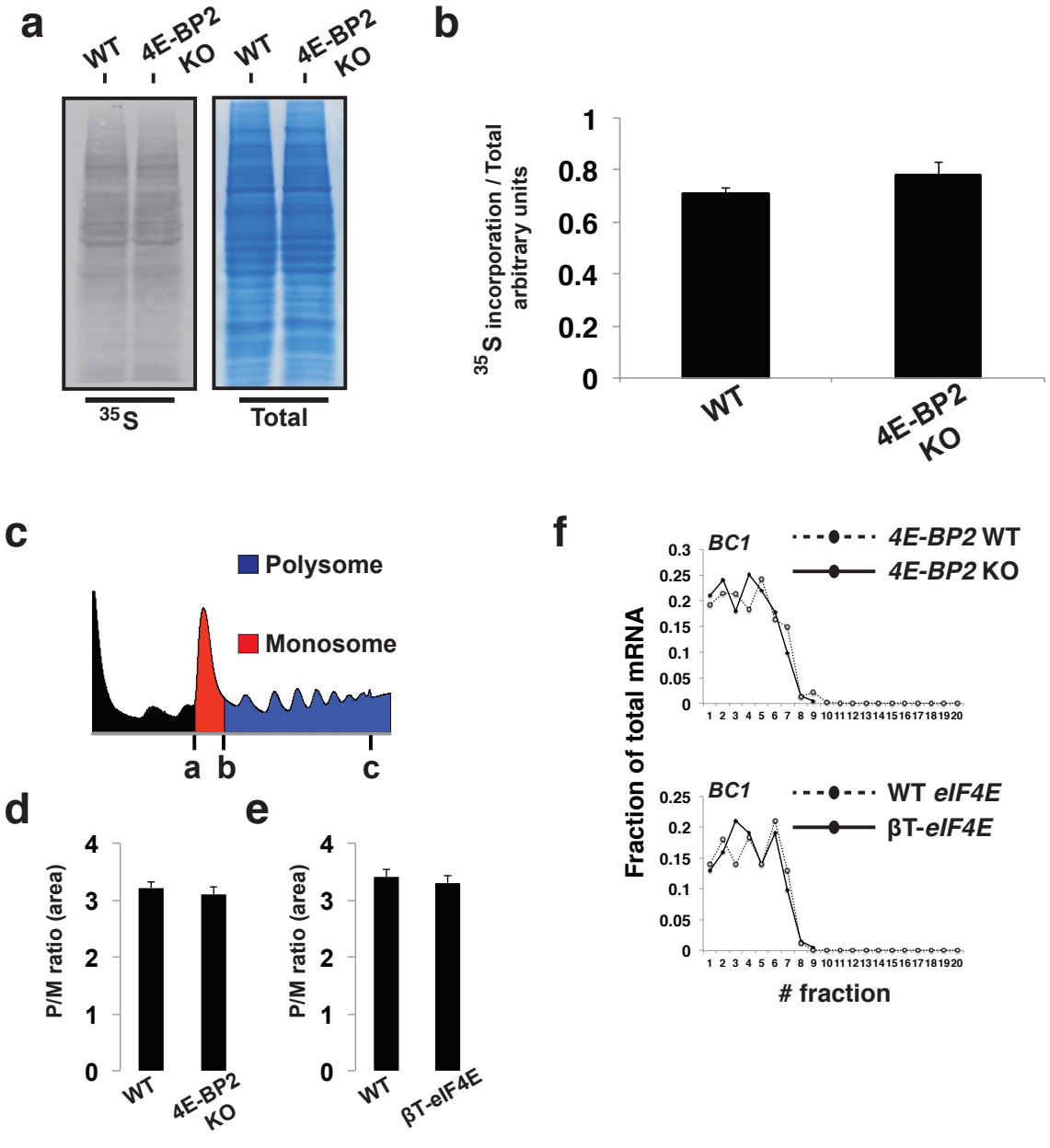

Supplementary Figure 5. General translation is not altered in *4E-BP2*-KO mice.
(a) Representative images of SDS-PAGE gel transferred to nitrocellulose measuring ^{35}S-Methionine incorporation from acute hippocampal slices (LEFT) and GelBlue stained SDS-PAGE gel of total protein loaded on gel (RIGHT) from *4E-BP2*-KO or WT littermate mice (n=3).
(b) Quantification of ^{35}S-Methionine incorporation normalized to total protein amount from (a). No changes in global translation are observed between WT-*4E-BP2*-KO ($p=0.214$), n=3; Student's *t*-test.
(c) Graphic depiction of the calculation of the P/M ratio (polysome to monosome) using the definite integral for the A254 absorbance function.

(d), (e) Quantification of P/M ratio from polysome profiles generated from hippocampal *4E-BP2*-KO, βT-*eIF4E* or WT lysates. No changes in the P/M ratio are observed between the examined genotypes (p=0.092, p=0.112 respectively); (n=4), Student's *t*-test.
(f) qRT-PCR analysis of different fractions of the polysome profile extracted RNA from *4E-BP2* WT and KO mice or from WT and βT-*eIF4E* mice. The fraction of total mRNA is shown for the different gradient fractions for *BC1,* a dendritic RNA. No detection in polysomal fractions is observed for *BC1* RNA (n=4) and no fraction shift between the indicated genotypes-statistics in Supplementary Table 4. All data are presented as mean ±SEM.

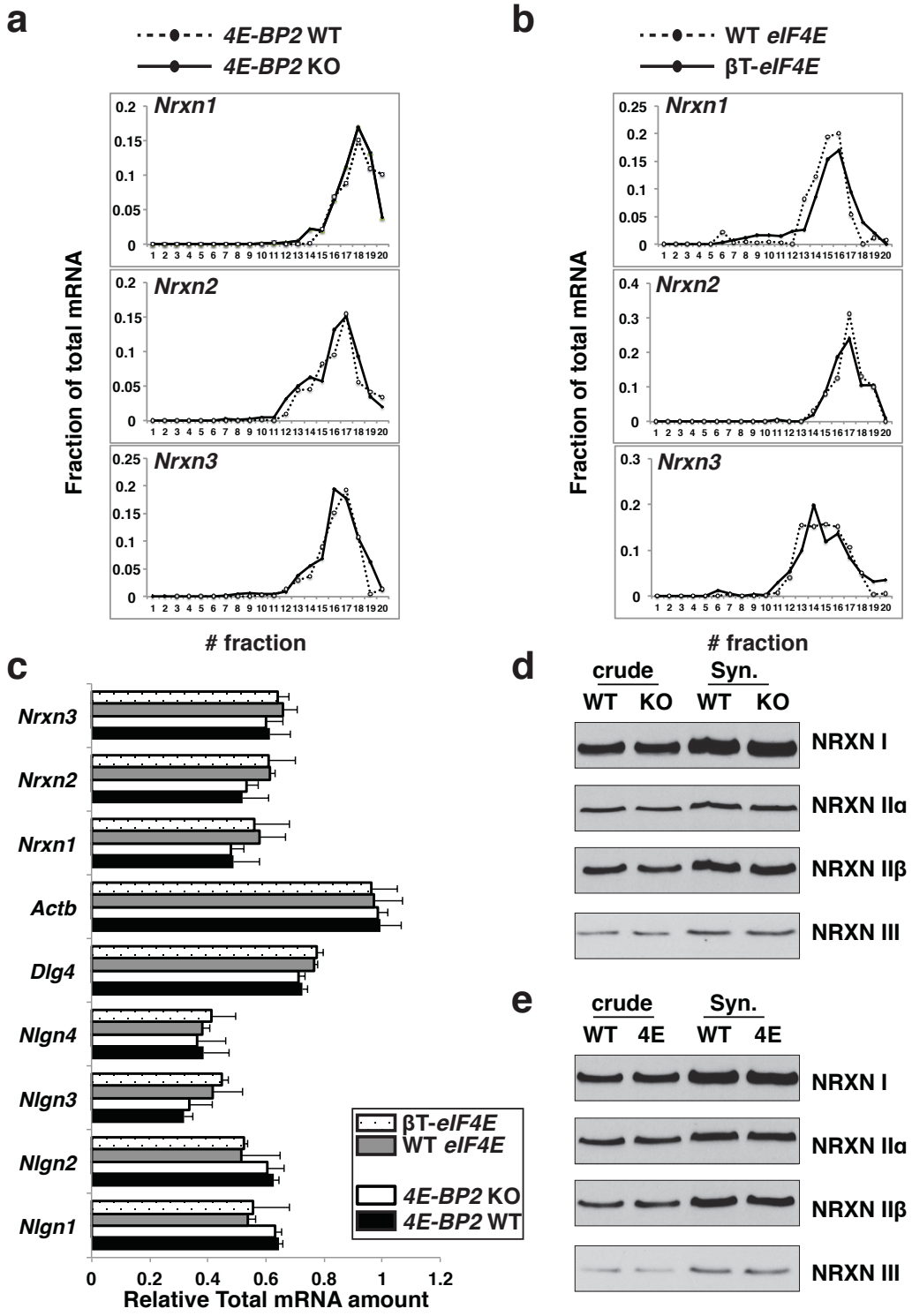

Supplementary Figure 6. Translational profiling using qRT-PCR and Western blot analysis of neurexins in *4E-BP2*-KO and βT-*eIF4E* mice.

(a) qRT-PCR analysis of RNA extracted from fractions of the polysome density gradient from *4E-BP2* WT and KO mice and (b) from WT and βT-*eIF4E* mice. Fraction of total mRNA is shown for the gradient fractions for *Nrxn1*, *2* and *3* (n=4 for *4E-BP2* WT and

KO, WT and βT-*eIF4E* mice). No shift in the distribution of *neurexin* mRNAs is observed.
(c) qRT-PCR analysis of total RNA in *4E-BP2* WT and KO, WT and βT-*eIF4E* mice. No change is observed in the amounts of *Nlgn*1, *2*, *3* and 4, *Dlg4*, *Actb*, *Nrxn1*, *2* and *3* mRNAs (n=4 for *4E-BP2* WT and KO, WT and βT-*eIF4E* mice).
(d-e) Western Blot analysis of crude and synaptosomal (Syn.) fractions of *4E-BP2* WT or *4E-BP2*-KO (D) and WT or βT-*eIF4E* (E) cortical lysates. Representative immunoblots are shown of lysates probed for neurexins (NRXN) 1, 2 and 3 (α and β isoforms). No change in protein amounts is observed (n=4). Student's *t*-test-in Supplementary Table 4. All data are presented as mean ±SEM.

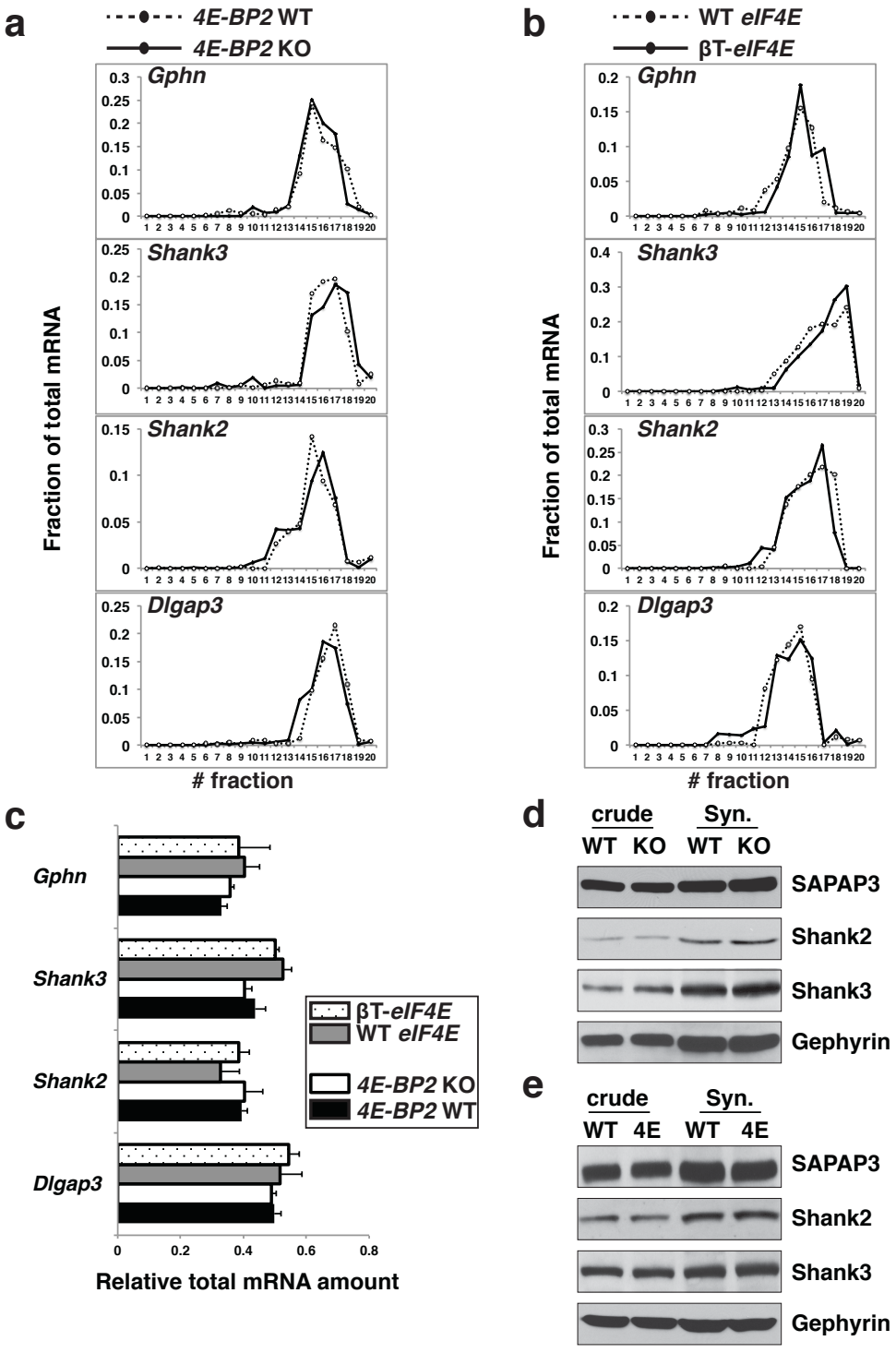

Supplementary Figure 7. Translational profiling using qRT-PCR and Western blot analysis of post-synaptic scaffolding proteins in *4E-BP2*-KO and βT-*eIF4E* mice. (a-b) qRT-PCR analysis of RNA extracted from fractions of the polysome density gradient from *4E-BP2* WT and KO mice and (b) from WT and βT-*eIF4E* mice. Fraction of total mRNA is shown for the gradient fractions for *Dlgap3*, *Shank2*, *Shank3* and *Gphn*

(n=4 for *4E-BP2* WT and KO, WT and βT-*eIF4E* mice). No shift in the distribution of any of the mRNAs is observed.
(c) qRT-PCR analysis of total RNA in *4E-BP2* WT and KO, WT and βT-*eIF4E* mice. No change is observed in the amounts of *Dlgap3*, *Shank2*, *Shank3* and *Gphn* mRNAs (n=4 for *4E-BP2* WT and KO, WT and βT-*eIF4E* mice).
(d-e) Western Blot analysis of crude and synaptosomal (Syn.) fractions of WT or *4E-BP2*-KO and (d) WT or βT-*eIF4E* hippocampal lysates (e). Representative immunoblots are shown of lysates probed for SAPAP3 (*Dlgap3*), Shank2, Shank3 and Gephyrin (*Gphn*). No change in protein expression is observed (n=4).
Student's *t*-test-in Supplementary Table 4.
All data are presented as mean ±SEM.

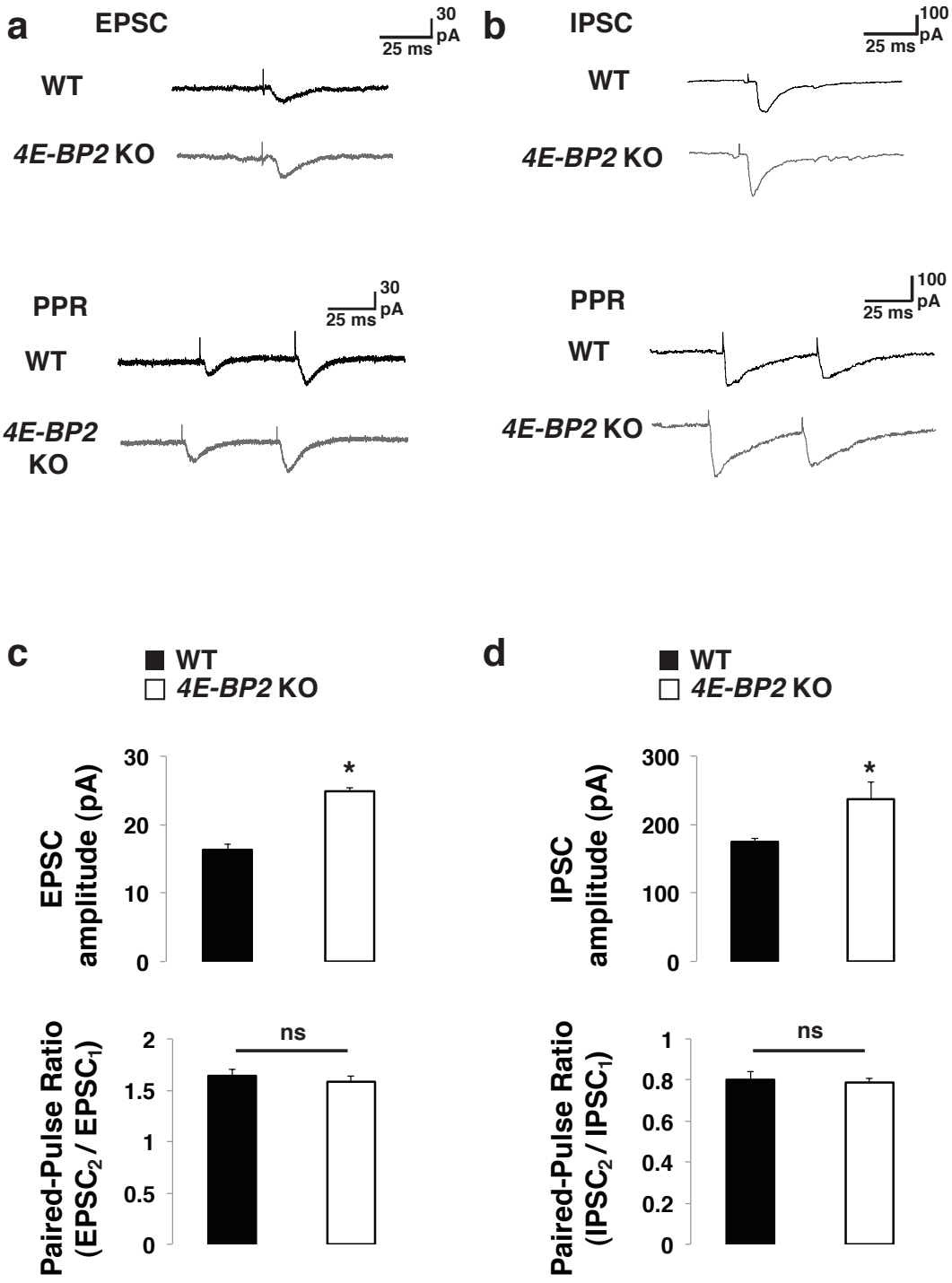

Supplementary Figure 8. Evoked synaptic transmission in *4E-BP2*-KO mice.
(a) Top traces are representative EPSCs evoked by minimal stimulation in CA1 pyramidal cells in acute slices from WT or *4E-BP2*-KO mice. Bottom traces EPSCs evoked by paired stimulation to measure paired-pulse ratio (PPR).
(b) Representative IPSCs evoked by minimal stimulation and paired-pulse responses from pyramidal cells from WT or *4E-BP2*-KO mice.

(c) EPSC amplitude evoked by minimal stimulation is increased in *4E-BP2*-KO mice ($p<0.001$), while the PPR is unaltered ($p=0.494$); n=4 for WT and KO groups.
(d) IPSC amplitude evoked by minimal stimulation is increased in *4E-BP2*-KO mice ($p=0.043$), while the PPR is unaltered ($p=0.695$); n=4 in WT and n=5 in KO, Student's *t*-test; *$p<0.05$. All data are presented as mean ±SEM.

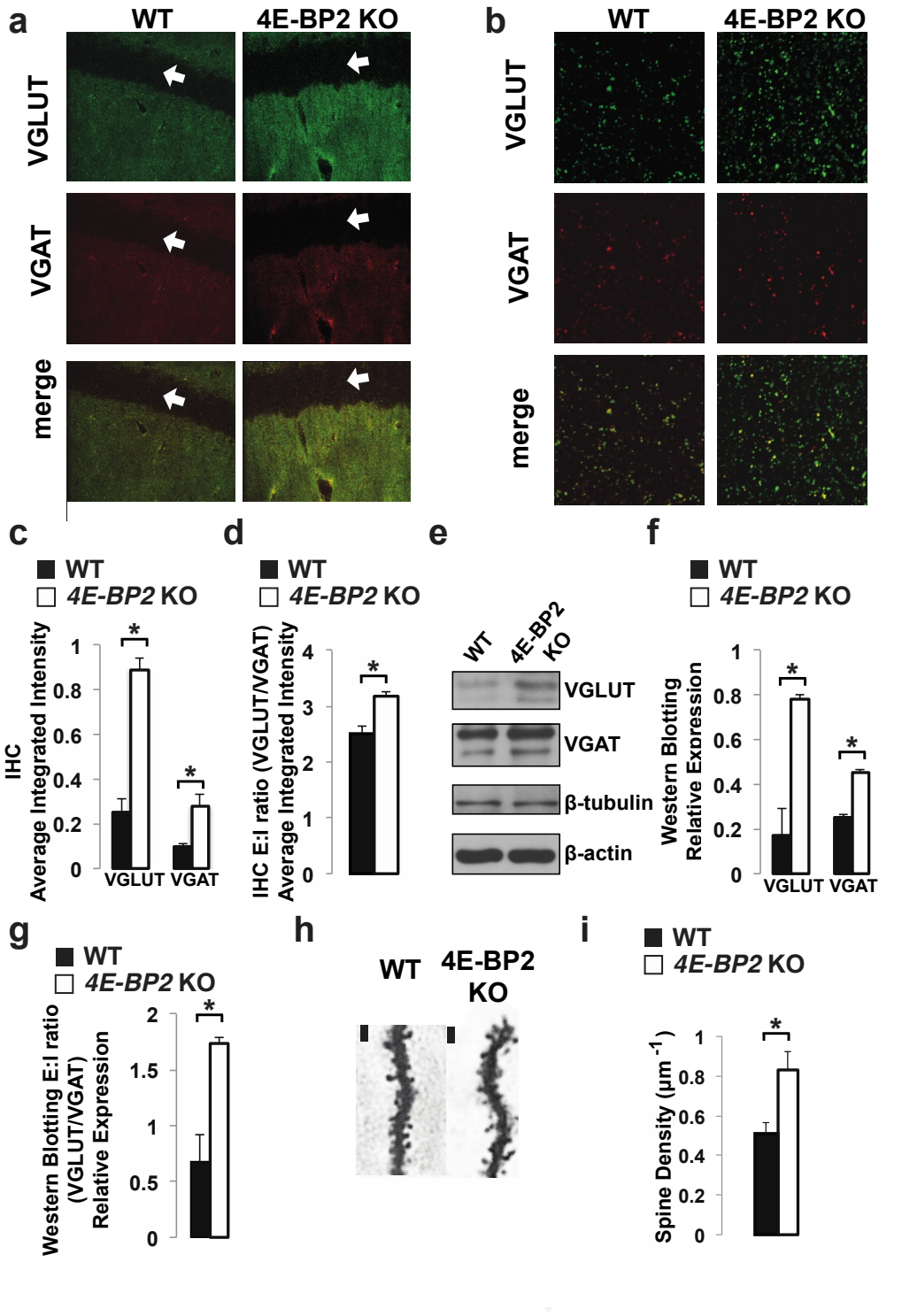

Supplementary Figure 9. Immunostaining and immunoblotting of excitatory & inhibitory synapses and dendritic spines in *4E-BP2*-KO mice.
(a) Representative confocal images from fixed hippocampal slices prepared from WT or *4E-BP2*-KO mice and (b) high magnification, stained with VGLUT or VGAT specific

antibodies and merged images. Arrows indicate the cell body layer of CA1 pyramidal neurons (not stained).
(c) Quantification of IHC staining for VGLUT or VGAT in hippocampal slices from WT or *4E-BP2*-KO mice from (b) * $p<0.05$, One-way ANOVA (arbitrary units).
(d) Excitation to inhibition ratio using average integrated intensity measurements from (c) (arbitrary units) * $p<0.05$, Student's *t*-test.
(e) Representative immunoblot images from synaptosomal fraction lysates prepared from WT or *4E-BP2*-KO hippocampi, probed with specific antibodies against the proteins depicted.
(f) Quantification of immunoblots for VGLUT or VGAT in hippocampal synaptosomes lysates from WT or *4E-BP2*-KO mice from (e) * $p<0.05$, Student's *t*-test (arbitrary units).
(g) Excitation to inhibition ratio using relative expression measurements from (f) (arbitrary units) * $p<0.05$, Student's *t*-test.
(h) Representative images of Golgi-stained hippocampal CA1 neuron dendrites, showing dendritic spines from WT or *4E-BP2*-KO mice; vertical black scale bars correspond to 3 μm.
(i) Quantification of spine density (spines per μm) for WT or *4E-BP2*-KO CA1 pyramidal neuron dendrites from (h) * $p<0.05$, Student's *t*-test. All data are presented as mean ±SEM.

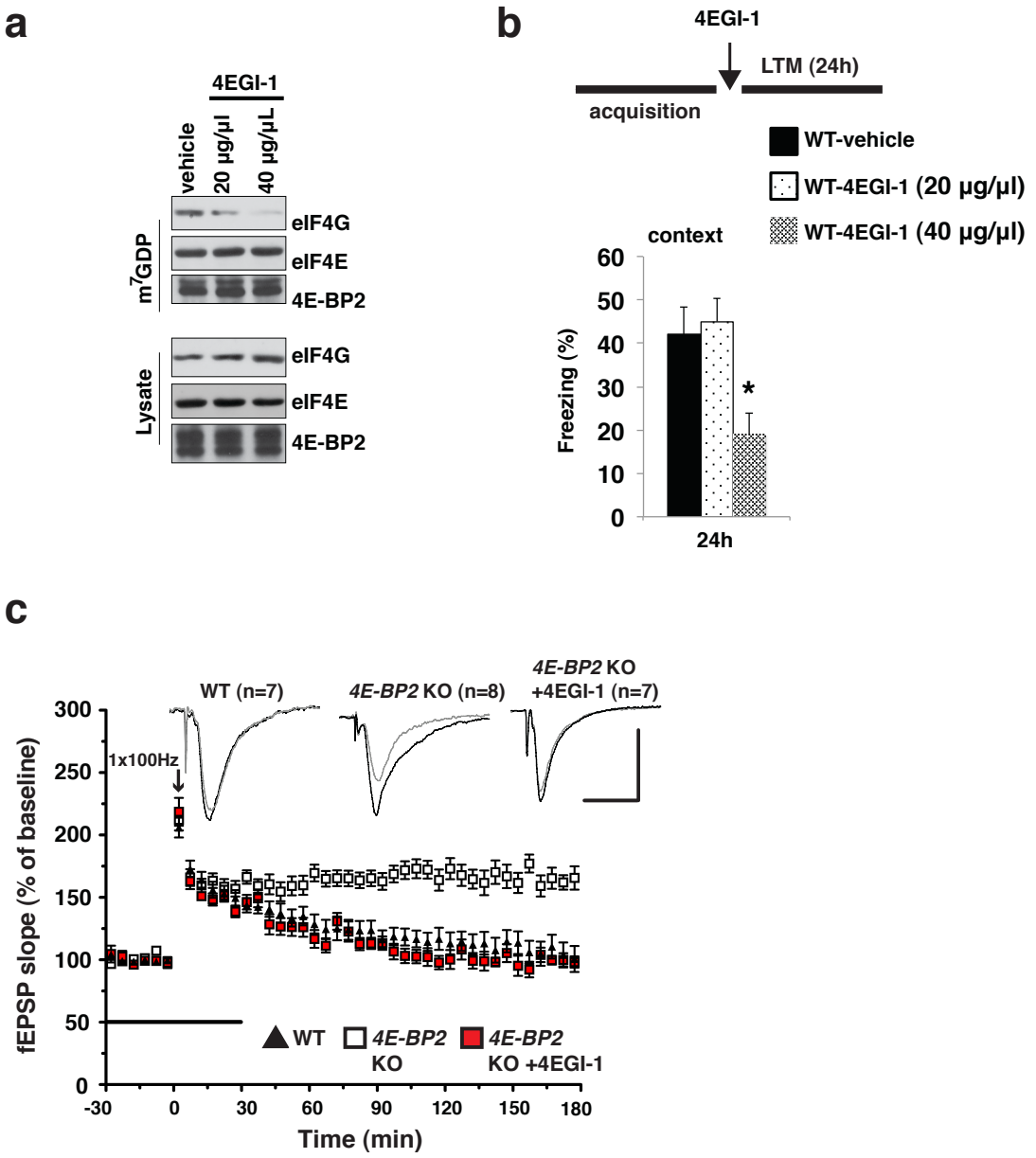

Supplementary Figure 10. 4EGI-1 blocks eIF4F complex formation, affects fear-conditioned memories and rescues E-LTP to L-LTP conversion in *4E-BP2*-KO mice. (a) Representative immunoblot images from total or m^{7}GDP-pulldown hippocampal lysates from WT mice, cannulated and infused with different concentrations of 4EGI-1, probed with antibodies specific to the indicated proteins.
(b) 4EGI-1 is infused after the acquisition phase of contextual fear conditioning. Long-Term Memory (LTM) is assessed 24h after acquisition; *$p<0.05$ n=6 mice for each group; One-way ANOVA and Tukey's posthoc test.
(c) Field recording experiments with 1 train tetanic stimulation in hippocampal slices from *4E-BP2*-KO and WT littermates treated with vehicle or 4EGI-1, showing that 4EGI-1 prevented the facilitation of L-LTP in *4E-BP2*-KO mice. Scale bar corresponds to 10 ms and 1 mV. Two-way ANOVA. All data are presented as mean ±SEM.

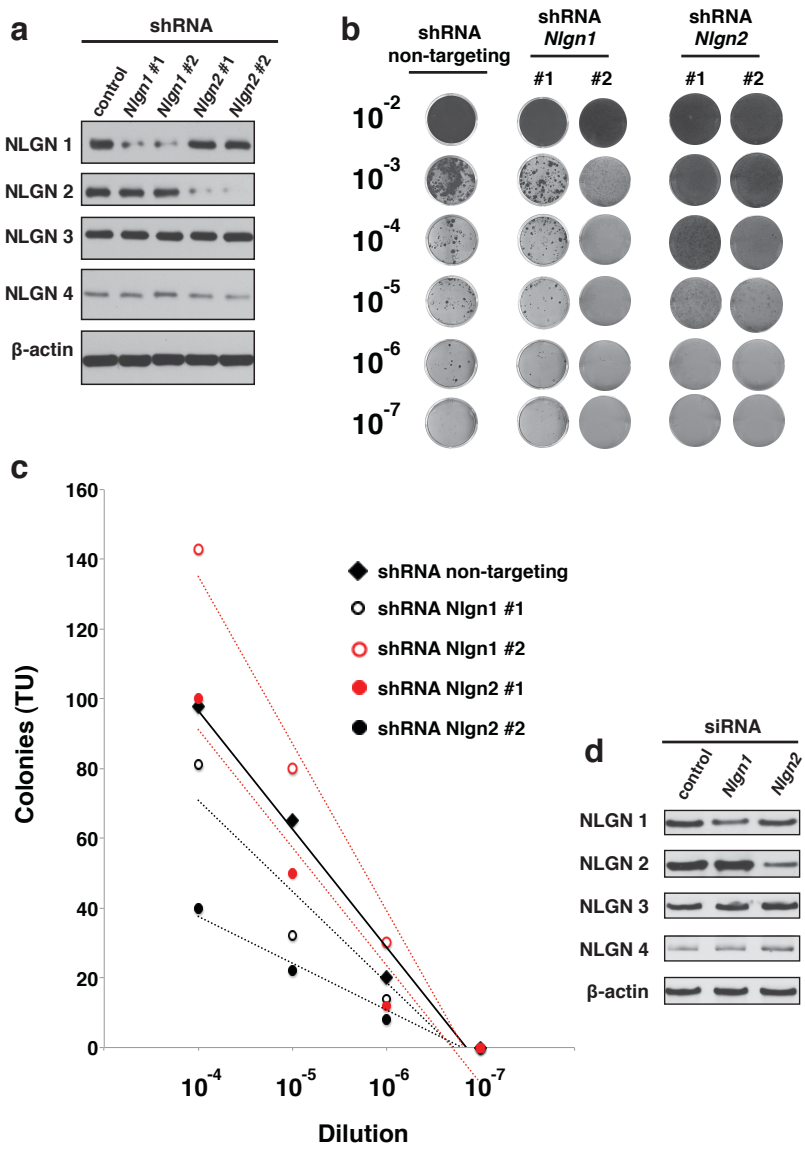

Supplementary Figure 11. Lentivirus-mediated knockdown of NLGN1 and 2.
(a) Western blot analysis of lysates from N2A cells infected with lentiviruses expressing different shRNAs against *Nlgn1, Nlgn2* or a non-targeting sequence. Reduced expression of NLGN 1 or NLGN2 is observed in cells infected with relevant shRNAs. No effect of *Nlgn1, 2* shRNAs on protein levels of NLGN 2, 3, 4 or b-actin.
(b) Colony formation to determine lentiviral titer. Representative images from N2A cells infected with different dilutions of lentiviruses encoding for shRNA #1, #2 against *Nlgn1*, shRNA #1,#2 against *Nlgn2* or non-targeting, stained with crystal violet.
(c) Quantification of transducing units per ml (TU/ml) of the lentiviruses in (b).
(d) Western blot analysis of lysates from N2A cells transiently transfected with siRNAs against *Nlgn1, Nlgn2* or a control siRNA (mix of si*Nlgn1* and si*Nlgn2* scrambled). Reduced expression of NLGN 1 or NLGN2 is observed in cells transfected with their respective siRNAs. No effect of *Nlgn1* or *2* siRNAs on protein levels of NLGN 3, 4 or b-actin.

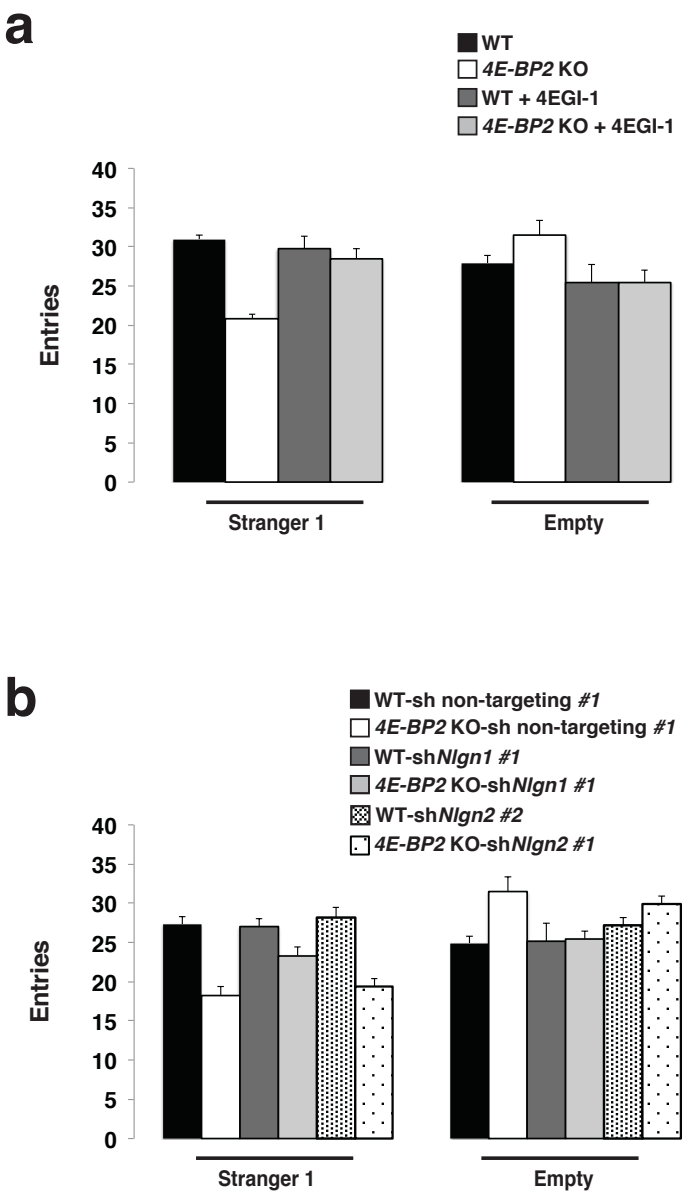

Supplementary Figure 12. Behavioral effects of knockdown of NLGN1, 2 with additional shRNAs *in vivo*.
Additional shRNAs were used for *Nlgn1* or *Nlgn2*. Knockdown of NLGN1 partially rescues the social interaction deficits of *4E-BP2*-KO mice, while knockdown of NLGN2 exacerbates the phenotype. n=12 for all groups, two-way ANOVA, with Bonferroni's post-hoc; *corresponds to a $p<0.05$-statistics in Supplementary Table 4. All data are presented as mean ±SEM.

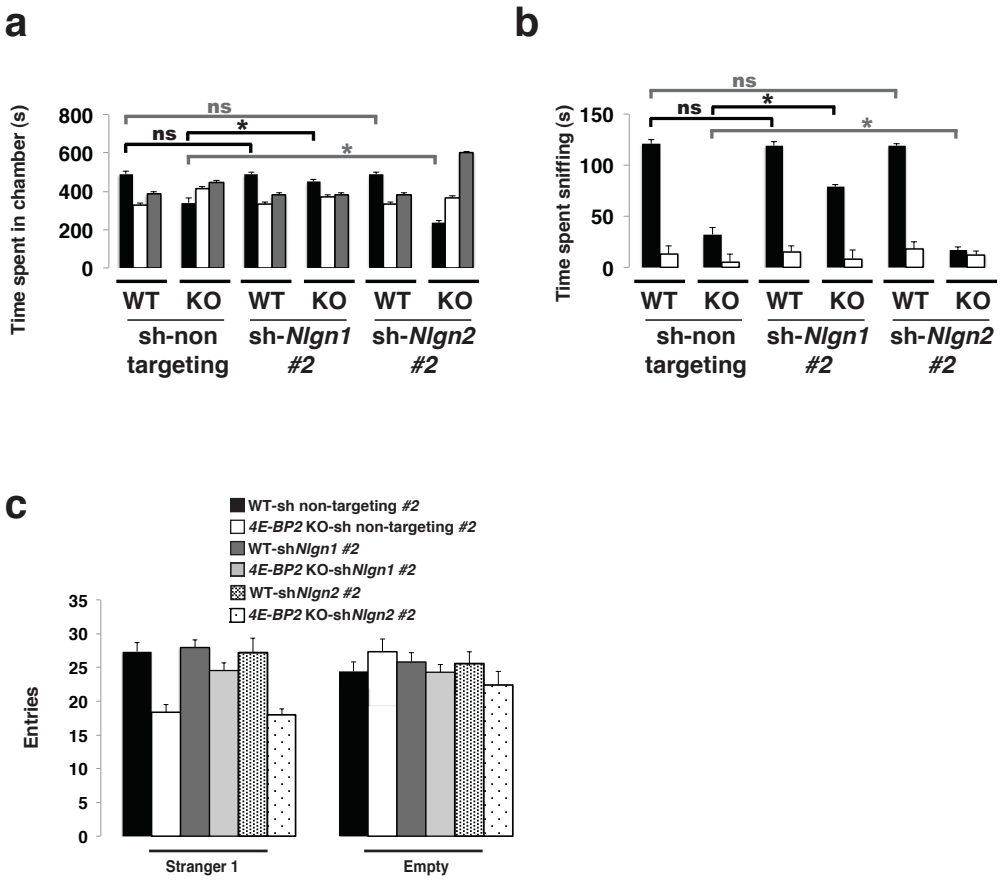

Supplementary Figure 13. Supplementary behavioral parameters rescued with 4EGI-1 or Nlgn1 or 2 knockdown in vivo.
(a-b) Effect of 4EGI-1 or vehicle (a) or *Nlgn1* or *Nlgn2* shRNAs on number of entries in WT or *4E-BP2*-KO mice; n=12 for all groups, two-way ANOVA, with Bonferroni's post-hoc test-in Supplementary Table 4. All data are presented as mean ±SEM.

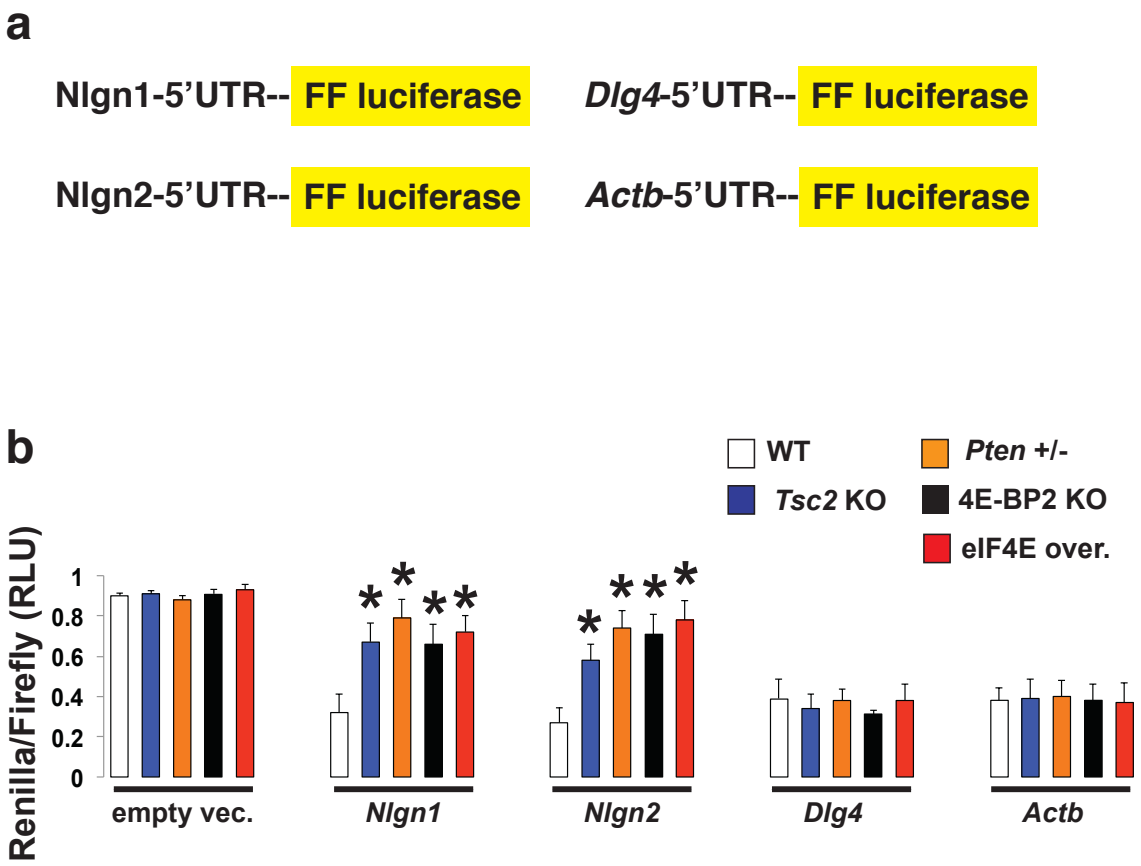

Supplementary Figure 14. Increased mTORC1 signaling leads to enhanced translation of *Nlgn* 5' UTRs.

(a) Reporter luciferase vectors with 5' UTRs of *Nlgn1, 2, Dlg4, Actb* cloned upstream of the firefly luciferase genes.

(b) Luminescence of firefly luciferase expressed as relative light units (normalized to renilla luciferase luminescence) for the depicted MEF lines. Nlgn 5' UTRs are translated more in cell lines with enhanced mTORC1 signaling (*Pten* +/-, *Tsc2* KO) or increased eIF4E dependent translation (*4E-BP2*-KO, eIF4E overexpression); one-way ANOVA; Bonferroni's post-hoc *p<0.001 (n=4).

All data are presented as mean ±SEM.

a

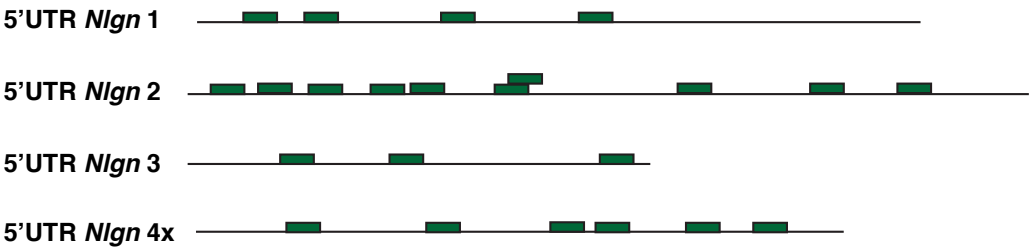

b

```
>nlgn1_w25_183        AUGGAAAACAGAAUGUUCAAUAGGA       (((((((((..))).)))))).... 
>nlgn1_w25_283        GAAGAUCUUUCAGAGCUUUUCUCGA       (((((((((..).))))))))....
>nlgn1_w25_41        AAGCUUGAGGCCACUCAAGUUCCAA       ((((((((((..))))))))))...
>nlgn1_w25_85         GGGCUCACUGGAGUGGCAGAUAUAG       ((((.((((..))))))))......
>nlgn2_w25_133      CCCGGCGGCGGCGCCCCGGGCGGCC       ((((((((((..))))))))))).
>nlgn2_w25_161     GCCUGGGCCUCGGCAGCCUCGGCGA        (((.(((((((..))))))))))..
>nlgn2_w25_17      UCUCUCUCUCCGAGGGGGGGGGGUC        ((((((((((..))))))))))).
>nlgn2_w25_223       GUGCGCGGUGUGCGGCGCGAGCUCA       ((((((((((..))))))))))...
>nlgn2_w25_451        UUGGAGGCGGCCGCCACCUACGUGC       ((((((((((..))))))))).....
>nlgn2_w25_514      GUGCCCACCGAGGACGGUCCGCUCA        ((((((((((..))))))))))).
>nlgn2_w25_51          GAGGGGGGGUCCCCCGAUCAGCAUG       ((((((((..)))))).))).......
>nlgn3_w25_87      GCUGUGUCUGGUGGGGCUGGCGGGG       .((((((((((..))))))))))
>nlgn3_w25_146       CUGAGGGAGUCCCCUUUCUGAAGCU       ((((((((((..))))))))).)..
>nlgn3_w25_299       AGUCUGCCUCUCCUGCCAGUCCCCC       ((((((((((..))))))))))...
>nlgn4x_w25_67         CUUGGCCUGGAGGCGAUAUGGGUGG       ((((((((..)))))).).).....
>nlgn4x_w25_168       GAGUUUUCAUAAGAAAUUGUCCCUG       ((((((((..)))))).)).....
>nlgn4x_w25_256       AAGGGAGGGCUGCCUCCUUGCAAUG       ((((((((..))))))))).....
>nlgn4x_w25_289     AGAAAACGGCUGUGCUUGUUCUUAA       ((((((((((..))))))))))).
>nlgn4x_w25_356    UCUACUGCUCCCUGGAAAGCCCUAU       ..((((((((((..))))))))))).
>nlgn4x_w25_404      CUUUGUCUCCUUGGAGCCACAUCAC       ((((((((((..))))))))).)..
```

c

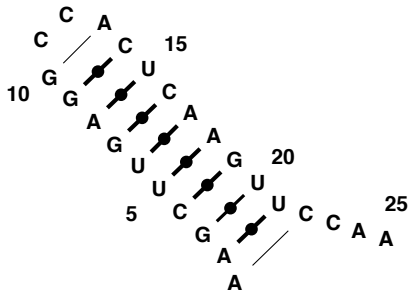

Supplementary Figure 15. Neuroligin 5'UTRs share a repeated, unique structural motif.

(a) Identification of a repeated hairpin in the 5'UTR of human *Nlgns*. We examined the *Nlgn* 5'UTRs for unique secondary (2D) structural motifs, absent from the group of postsynaptic mRNA 5'UTRs [which were not affected by increased cap-dependent translation (control group)]. We predicted the 2D structures of all subsequences of 15 to

80 nucleotides (nt) using the MC-Fold energy model[41]. We defined the structural similarity between two windows using statistics of the base pairs and unpaired nucleotides found in the predicted 2D structures. We applied hierarchical clustering on all windows using the calculated structural similarity. This process identified three clusters with 25-nt windows present in all *Nlgns* but not in any 5'UTRs of the control group. We used the MC-Cons software to identify among the predicted secondary structures, those optimizing their structural alignments. The structures of one cluster are shown in green.
(b) Sequence and structural alignment of the repeated structural element. The structure among all predictions selected by MC-Cons is shown for each repeat. Dot-Bracket Notation: dotted correspond to unpaired nucleotides, while matching parenthesized positions depict base-paring nucleotides.
(c) Secondary structure selected by MC-Cons for the repeat at position 41 in *Nlgn1*.

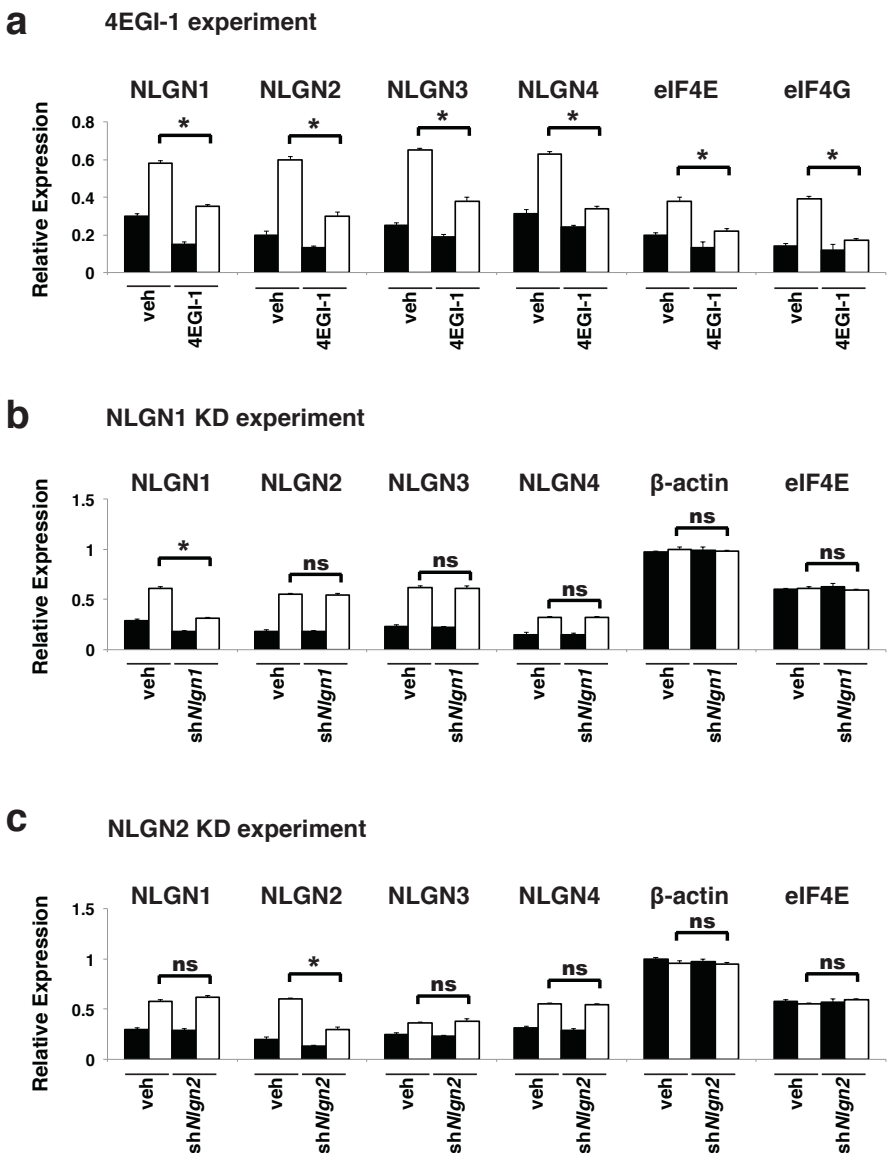

Supplementary Figure 16. Quantification of the effects of 4EGI-1 application or NLGN knockdown on different proteins vs genotype.

(a) Relative expression of NLGN1, 2, 3 and 4, cap-bound eIF4E and eIF4G in vehicle or 4EGI-1 treated WT or KO mice. A significant interaction between genotype, expression and treatment was observed [$F(5,96)=21.32$, $p<0.030$]. Results are summarized in Supplementary Table 4; n=4 for each group; *$p<0.05$ two-way ANOVA with Bonferroni's post-hoc.

(b-c) Relative expression of NLGN1, 2, 3 and 4, β-actin or eIF4E in control shRNA or sh*Nlgn1* or sh*Nlgn2* infused WT or KO mice. A significant interaction between genotype, expression and treatment was observed for the *Nlgn1* knockdown group [$F(5,96)=32.89$, $p<0.030$] or the *Nlgn2* [$F(5,96)=12.34$, $p<0.030$]; n=4 for each group; *$p<0.05$; two-way ANOVA with Bonferroni's post-hoc. All data are presented as mean ±SEM.

Supplementary Table 1. Mouse models of neuroligins.

	Behavior	References
Nlgn1 KO	• Minimal differences in reciprocal social interactions	Chubykin et al.
	• Minimal differences in sociability	Chubykin et al.
	• Minimal differences in preference for social novelty	Chubykin et al.
	• Impaired nest-building behavior	Chubykin et al.
	• Impaired spatial memory	Chubykin et al.
Nlgn2 KO	• Increased anxiety-like behavior in open arena	Blundell et al.
	• Increased anxiety-like behavior in light/dark box	Blundell et al.
	• No differences in social interaction and social learning	Blundell et al.
	• No differences in preference for social novelty	Blundell et al.
Nlgn3 KO	• No differences in reciprocal social interactions	Radyushkin et al.
	• Reduced preference for social novelty	Radyushkin et al.
	• Reduction in number of ultrasonic vocalizations in adult males	Radyushkin et al.
	• Olfactory deficiency (latency to find buried food)	Radyushkin et al.
Nlgn3 R451C	• No changes in locomotor activity, motor coordination, and anxiety-related behaviors	Tabuchi et al.
	• Impaired social learning	Tabuchi et al.
	• Impaired performance in the social versus inanimate preference test	Tabuchi et al.
	• Enhanced spatial learning	Tabuchi et al.
	• No differences in reciprocal social interactions	Chadman et al.
	• No differences in sociability	Chadman et al.
	• No differences in preference for social novelty	Chadman et al.
	• Reduced ultrasonic vocalizations	Chadman et al.
	• Social interaction impairments	Etherton et al.
Nlgn3 R704C	• No changes in locomotor activity, motor coordination, and anxiety-related behaviors	Tabuchi et al.
	• Impaired social learning	Tabuchi et al.
	• Impaired performance in the social versus inanimate preference test	Tabuchi et al.
Nlgn4 KO	• Reduced reciprocal social interaction	Jamain et al.
	• Reduced sociability	Jamain et al.
	• Impaired preference for social novelty	Jamain et al.
	• Reduced ultrasonic vocalizations	Jamain et al.
Nlgn1 Tg (overexpression)	•Impaired memory acquisition in +Watermaze and Morris Watermaze	Dalhaus et al.
	•Impaired spatial memory	Dalhaus et al.
Nlgn2 Tg (overexpression)	• Jumping stereotypy	Hines et al.
	• Increased anxiety-related behavior	Hines et al.
	• Reduced reciprocal social interactions	Hines et al.
	• Reduced social approach	Hines et al.

	Electrophysiology	References
Nlgn1 KO	• Impaired theta-burst LTP in CA1	Blundell et al.
	• Reduced EPSCs, without affecting IPSCs	Chubykin et al.
Nlgn2 KO	• Depression of evoked IPSCs in cortex	Chubykin et al.
	• Shift of E/I ratio towards excitation in Dentate Gyrus by reduction of inhibition	Jedlicka et al.
Nlgn3 KO	• No difference in spontaneous or evoked inhibitory synaptic transmission in the somatosensory cortex	Tabuchi et al.
Nlgn3 R451C	• Increased spontaneous and evoked inhibitory synaptic transmission in the somatoensory cortex, with no effect on excitation	Tabuchi et al.
	• Increased excitatory synaptic transmission in CA1	Etherton et al.
	• Increased LTP	Etherton et al.
Nlgn3 R704C	• Increased spontaneous and evoked inhibitory synaptic transmission in the somatoensory cortex, with no effect on excitation	Tabuchi et al.
	• Increased excitatory synaptic transmission in CA1	Etherton et al.
	• Increased LTP	Etherton et al.
Nlgn4 KO	• Slower kinetics of glycinergic mIPSCs in RGCs	Hoon et al.
	• No change in GABAergic mIPSCs in RGCs	Hoon et al.
Nlgn1 Tg (overexpression)	• Impaired LTP in CA1	Dalhaus et al.
	• Increased basal excitation and unaltered inhibition in the hippocampus	Dalhaus et al.
Nlgn2 Tg (overexpression)	• Increased mIPSC frequency in pyramidal neurons of the PFC	Hines et al.
	• Seizure spiking activity recorded with EEG	Hines et al.

Supplementary Table 2. Translational profiling of ASD related mRNAs and controls in *4E-BP2*-KO and βT-*eIF4E* mice

Gene	shifts in 4E-BP2 KO	shifts in βT-eIF4E
Nlgn1	✓	✓
Nlgn2	✓	✓
Nlgn3	✓	✓
Nlgn4	✓	✓
Nrxn1	✗	✗
Nrxn2	✗	✗
Nrxn3	✗	✗
Dlg4	✗	✗
Dlgap3	✗	✗
Shank2	✗	✗
Shank3	✗	✗
Gphn	✗	✗
Cdh9	✗	✗
Cdh10	✗	✗
Gabrb3	✗	✗
Itgb3	✗	✗
En2	✗	✗
MeCP2	✗	✗
A2bp1	✗	✗
Gapdh	✗	✗
Gfap	✗	✗
Actb	✗	✗
Ctnna3	✗	✗

Supplementary Table 3. Primers used for qRT-PCR.

Primer name	Primer sequence (5'-3')	NCBI accession #
Fw-Nlgn1	ACAGGAGAACATCGTTTCCAGCCT	NM_138666.3
Rev-Nlgn1	ATACAGGAGCAAACTGAGTGGCGT	
Fw-Nlgn2	ACTATCTTTGGGTCTGGTGC	NM_198862.2
Rev-Nlgn2	ATGAGCATGTCGTAGTTGAGG	
Fw-Nlgn3	GTGAAATCCTGGGTCCTGTG	NM_172932.3
Rev-Nlgn3	GTCTTCATCTTCATCCCCGTC	
Fw-Nlgn4	AGGACGCGCACGTGATCTCTTAAT	EU350930
Rev-Nlgn4	TTTCTGAGGCAGTGGGATGACTGT	
Fw-Dlg4	ATCGGTGACGACCCATCCATCTTT	NM_007864.3
Rev-Dlg4	TCCCGGACATCCACTTCATTGACA	
Fw-Dlg2	TAAAGCAGTGGAAGCCCTCAAGGA	NM_011807.3
Rev-Dlg2	ACAGTCTCCAATATGGGTCGCCTT	
Fw-Dlgap3	TGGATGGACAGTCAGTCAAGCGAA	NM_198618.4
Rev-Dlgap3	AGTGATAAGTCCTGGCTTTGGCCT	
Fw-Shank2	AGAAGAGGACACGGATGGCTTTGT	NM_001081370.2
Rev-Shank2	ATGACATTTGCCTTTGGGCCTGAG	
Fw-Shank3	TAGCCTTCAAGACGCGCTCAACTA	NM_021423.3
Rev-Shank3	TCTGGGCATAAACTCTCCGCTTGT	
Fw-Gphn	ATGATCCTCACCAACCACGACCAT	NM_145965.2
Rev-Gphn	TGCCGATATAGTCCCACCCAACAA	
Fw-Nrxn1	GCAGTCGCCTTATCCTTAGAC	NM_020252.3
Rev-Nrxn1	GGCTGATTCGCTTTATGTTTAGG	
Fw-Nrxn2	CAATGGGTTGTTGCTCTTCAGCCA	NM_001205234.1
Rev-Nrxn2	ATTCACCATCATTGACCTTGCGGC	
Fw-Nrxn3	ATGGTGCGGTCTCCTTGGTCATTA	NM_001198587.1
Rev-Nrxn3	TGCCGAAGATTGCGTGTCACTTTG	
Fw-Cdh9	ACGAAAGACCTGTACACAGCCAGT	NM_009869.1
Rev-Cdh9	ATTATGCCTGATTCCGGGTCCACT	
Fw-Cdh10	GATGGAGATGGCACGGATATG	NM_009865.2
Rev-Cdh10	GAGGATCGACTGAAAACAGGAG	
Fw-Gabrb3	CTCCCACAGTTCTCCATTGTAG	NM_008071.3
Rev-Gabrb3	GGATTGAGGGCATATACGTCTG	
Fw-Itgb3	AAGAACGAGGATGACTGTGTC	NM_016780.2
Rev-Itgb3	ATATTGGTGAAGGTGGAGGTG	
Fw-En2	CGCTTGGGTCTACTGCAC	NM_010134.3
Rev-En2	CCCGTGGCTTTCTTGATTTTG	
Fw-MeCP2	CAGGCAAAGCAGAAACATCAG	NM_001081979.1
Rev-MeCP2	GTCAAAATCATTAGGGTCCAAGG	
Fw-A2bp1	ACACAGAAAGCAAGTCCCAG	BC059002.1
Rev-A2bp1	CAATTTCTCCCTCGCCCTATC	
Fw-Gapdh	TCAACAGCAACTCCCACTCTTCCA	NM_008084.2
Rev-Gapdh	ACCCTGTTGCTGTAGCCGTATTCA	
Fw-Gfap	GGAAATTGCTGGAGGGCGAAGAAA	NM_001131020.1
Rev-Gfap	TGGTGAGCCTGTATTGGGACAACT	
Fw-Actb	TGTGATGGTGGGAATGGGTCAGAA	NM_007393.3
Rev-Actb	TGTGGTGCCAGATCTTCTCCATGT	
Fw-Ctnna3	GCGCAGGTTTCTCAGGAG	NM_001164376.1
Rev-Ctnna3	CACAGTGAACGTTTGGATCTG	
Fw-Grik2	GTTCCTCACATACAGACCCG	NM_001111268.1
Rev-Grik2	GCCCCTCTTCATCTCTTTCAG	
Fw-Cntnap2	CAGATCAGTGCCATTGCAACCCAA	NM_001004357.2
Rev-Cntnap2	AGGGTTTCCAGTTTCTCCCTGTGT	
Fw-Cacna1c	AATGATTCGGGCCTTTGTTCAGCC	NM_009781.3
Rev-Cacna1c	TACCACCTTGCCCTTGAACTTCCT	
Fw-Bc1	TTTAGCTCAGTGGTAGAGCGCTTG	NR_038088
Rev-Bc1	GGTTGTGTGTGCCAGTTACCTTGT	

Supplementary References

1. Chubykin, A. A. *et al.* Activity-dependent validation of excitatory versus inhibitory synapses by neuroligin-1 versus neuroligin-2. *Neuron* **54**, 919-931, doi:10.1016/j.neuron.2007.05.029 (2007).
2. Blundell, J. *et al.* Increased anxiety-like behavior in mice lacking the inhibitory synapse cell adhesion molecule neuroligin 2. *Genes Brain Behav* **8**, 114-126, doi:GBB455 [pii]
10.1111/j.1601-183X.2008.00455.x (2009).
3. Blundell, J. *et al.* Neuroligin-1 deletion results in impaired spatial memory and increased repetitive behavior. *The Journal of neuroscience : the official journal of the Society for Neuroscience* **30**, 2115-2129, doi:10.1523/JNEUROSCI.4517-09.2010 (2010).
4. Jamain, S. *et al.* Reduced social interaction and ultrasonic communication in a mouse model of monogenic heritable autism. *Proceedings of the National Academy of Sciences of the United States of America* **105**, 1710-1715, doi:10.1073/pnas.0711555105 (2008).
5. Radyushkin, K. *et al.* Neuroligin-3-deficient mice: model of a monogenic heritable form of autism with an olfactory deficit. *Genes, brain, and behavior* **8**, 416-425, doi:10.1111/j.1601-183X.2009.00487.x (2009).
6. Tabuchi, K. *et al.* A neuroligin-3 mutation implicated in autism increases inhibitory synaptic transmission in mice. *Science* **318**, 71-76, doi:10.1126/science.1146221 (2007).
7. Etherton, M. R., Tabuchi, K., Sharma, M., Ko, J. & Sudhof, T. C. An autism-associated point mutation in the neuroligin cytoplasmic tail selectively impairs AMPA receptor-mediated synaptic transmission in hippocampus. *The EMBO journal* **30**, 2908-2919, doi:10.1038/emboj.2011.182 (2011).
8. Etherton, M. *et al.* Autism-linked neuroligin-3 R451C mutation differentially alters hippocampal and cortical synaptic function. *Proceedings of the National Academy of Sciences of the United States of America* **108**, 13764-13769, doi:10.1073/pnas.1111093108 (2011).
9. Dahlhaus, R. & El-Husseini, A. Altered neuroligin expression is involved in social deficits in a mouse model of the fragile X syndrome. *Behavioural brain research* **208**, 96-105, doi:10.1016/j.bbr.2009.11.019 (2010).
10. Hines, R. M. *et al.* Synaptic imbalance, stereotypies, and impaired social interactions in mice with altered neuroligin 2 expression. *The Journal of neuroscience : the official journal of the Society for Neuroscience* **28**, 6055-6067, doi:10.1523/JNEUROSCI.0032-08.2008 (2008).
11. Dahlhaus, R. *et al.* Overexpression of the cell adhesion protein neuroligin-1 induces learning deficits and impairs synaptic plasticity by altering the ratio of excitation to inhibition in the hippocampus. *Hippocampus* **20**, 305-322, doi:10.1002/hipo.20630 (2010).
12. Hoon, M. *et al.* Neuroligin 2 controls the maturation of GABAergic synapses and information processing in the retina. *The Journal of neuroscience : the official journal of the Society for Neuroscience* **29**, 8039-8050, doi:10.1523/JNEUROSCI.0534-09.2009 (2009).

13. Hoon, M. *et al.* Neuroligin-4 is localized to glycinergic postsynapses and regulates inhibition in the retina. *Proceedings of the National Academy of Sciences of the United States of America* **108**, 3053-3058, doi:10.1073/pnas.1006946108 (2011).
14. Budreck, E. C. & Scheiffele, P. Neuroligin-3 is a neuronal adhesion protein at GABAergic and glutamatergic synapses. *The European journal of neuroscience* **26**, 1738-1748, doi:10.1111/j.1460-9568.2007.05842.x (2007).
15. Lui, L. *et al.* Synaptic localization of neuroligin 2 in the rodent retina: comparative study with the dystroglycan-containing complex. *Journal of neuroscience research* **88**, 837-849, doi:10.1002/jnr.22258 (2010).
16. Poulopoulos, A. *et al.* Neuroligin 2 drives postsynaptic assembly at perisomatic inhibitory synapses through gephyrin and collybistin. *Neuron* **63**, 628-642, doi:10.1016/j.neuron.2009.08.023 (2009).